

# Lateral flow immunoassay for rapid and sensitive detection of dsRNA contaminants in *in vitro*-transcribed mRNA products

Dengwang Luo,<sup>1,2,11</sup> Zhanfeng Wu,<sup>3,4,11</sup> Daming Wang,<sup>5,6,7</sup> Jieli Zhang,<sup>7</sup> Fei Shao,<sup>4,8</sup> Shuo Wang,<sup>8</sup> Stefano Cestellos-Blanco,<sup>9</sup> Dawei Xu,<sup>2</sup> and Yuhong Cao<sup>2,10</sup>

<sup>1</sup>Frontier Science Center for Synthetic Biology and Key Laboratory of Systems Bioengineering (Ministry of Education), School of Chemical Engineering and Technology, Tianjin University, Tianjin 300072, China; <sup>2</sup>CAS Key Laboratory for Biological Effects of Nanomaterials and Nanosafety, National Center for Nanoscience and Technology, Chinese Academy of Sciences, Beijing 100190, China; <sup>3</sup>Beijing National Laboratory for Molecular Sciences, Key Laboratory of Molecular Nanostructure and Nanotechnology, CAS Research/Education Center for Excellence in Molecular Sciences, Institute of Chemistry, Chinese Academy of Sciences, Beijing 100190, China; <sup>4</sup>University of Chinese Academy of Sciences, Beijing 100049, China; <sup>5</sup>Academy for Engineering and Technology, Fudan University, Shanghai 200433, China; <sup>6</sup>Suzhou Institute of Biomedical Engineering and Technology (SIBET), Chinese Academy of Sciences, Suzhou, Jiangsu 215163, China; <sup>7</sup>Anbio Biotechnology Company, Xiamen, Fujian 361026, China; <sup>8</sup>CAS Key Laboratory of Pathogenic Microbiology and Immunology, Institute of Microbiology, Chinese Academy of Sciences, Beijing 100101, China; <sup>9</sup>Department of Materials Science and Engineering, University of California, Berkeley, Berkeley, CA 94720, USA; <sup>10</sup>School of Nanoscience and Technology, University of Chinese Academy of Sciences, Beijing 100049, China

**High purity is essential in mRNA-based therapeutic applications. A major contaminant of *in vitro*-transcribed (IVT) mRNA manufacturing is double-stranded RNA (dsRNA), which can induce severe anti-viral immune responses. Detection methods, such as agarose gel electrophoresis, ELISA, and dot-blot assay, are used to detect the existence of dsRNA in IVT mRNA products. However, these methods are either not sensitive enough or time-consuming. To overcome these challenges, we develop a rapid, sensitive, and easy-to-implement colloidal gold nanoparticle-based lateral flow strip assay (LFSA) with sandwich format for the detection of dsRNA from IVT process. dsRNA contaminant can be determined visually on the test strip or quantitatively with a portable optical detector. This method allows for a 15 min detection of N1-methyl-pseudouridine (m1Ψ)-containing dsRNA with a detection limit of 69.32 ng/mL. Furthermore, we establish the correlation between the LFSA test results and the immune response caused by dsRNA in mice. The LFSA platform allows the rapid, sensitive, and quantitative monitoring of purity in massive IVT mRNA products and aids for the prevention of immunogenicity by dsRNA impurities.**

transcription.<sup>7</sup> dsRNA can be recognized by endosomal membrane-bound Toll-like receptor-3 (TLR-3) and cytosolic RNA sensors such as melanoma differentiation-associated protein 5 (MDA5) and retinoic acid-inducible gene I (RIG-I).<sup>8,9</sup> dsRNA immune activation results in the up-regulation of various pro-inflammatory cytokines,<sup>10</sup> and cell death,<sup>11</sup> which can lead to patient morbidity. Therefore, to improve the quality of mRNA translation,<sup>12</sup> and minimize adverse effects, it is critical to carefully monitor *in vitro*-transcribed (IVT) mRNA products and confirm the removal of dsRNA after purification.

Agarose gel electrophoresis, ELISA, and dot-blot assay are well-established methods for detecting dsRNA contaminants in IVT. Agarose gel electrophoresis can be used for dsRNA detection, but it has low sensitivity.<sup>13</sup> ELISA using antibodies has been applied for determination of dsRNA concentration in total RNA because of their high sensitivity and reliability.<sup>14</sup> However, conventional ELISA is a multi-step process and requires hours of operation. Dot-blot assay is the other approach frequently used to detect dsRNA contaminant in mRNA. This method is also based on specific monoclonal antibody (mAb) recognition of dsRNA.<sup>15</sup> Similar to ELISA, this approach is

## INTRODUCTION

mRNA has gained significant worldwide attention as a novel active ingredient in vaccines and gene therapies.<sup>1,2</sup> The increasing demand for mRNA molecules has compelled mRNA manufacturers to quickly scale up production capacity while maintaining high mRNA quality.<sup>3,4</sup> *In vitro* transcription by T7 polymerase is the standard procedure to synthesize mRNA.<sup>5</sup> However, this procedure may introduce double-stranded RNA (dsRNA) contaminants from random priming of abortive transcripts,<sup>5</sup> turn-around transcription,<sup>6</sup> and antisense

Received 8 July 2022; accepted 4 April 2023;  
<https://doi.org/10.1016/j.omtn.2023.04.005>

<sup>11</sup>These authors contributed equally

**Correspondence:** Dawei Xu, CAS Key Laboratory for Biological Effects of Nanomaterials and Nanosafety, National Center for Nanoscience and Technology, Chinese Academy of Sciences, Beijing 100190, China.  
**E-mail:** [xudw@nanoctr.cn](mailto:xudw@nanoctr.cn)

**Correspondence:** Yuhong Cao, CAS Key Laboratory for Biological Effects of Nanomaterials and Nanosafety, National Center for Nanoscience and Technology, Chinese Academy of Sciences, Beijing 100190, China.  
**E-mail:** [caoyh@nanoctr.cn](mailto:caoyh@nanoctr.cn)



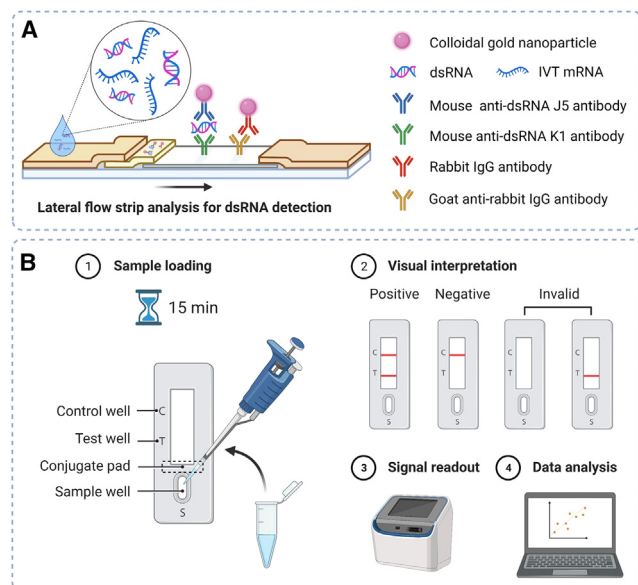


**Figure 1. The LFSA device for dsRNA detection**

(A) The principle of lateral flow strip assay. (B) The testing process of the LFSA for dsRNA detection.

complicated and requires over 4 h to complete. Additionally, it may cause false-positive result because of nonspecific adsorption of other substances by the membrane.<sup>16,17</sup> Given the technical challenges of detecting dsRNA, there is a pressing need to develop a rapid, simple-to-use, quantitative, and sensitive assay for detecting dsRNA.

Lateral flow strip assay (LFSA) is a well-established method for rapid detection, and is commonly used in disease diagnosis,<sup>18,19</sup> food safety,<sup>20</sup> and environmental monitoring.<sup>21</sup> As opposed to other detection methods, LFSA has various practical advantages,<sup>22,23</sup> including rapid on-site detection, simple operation, straightforward result interpretation, low cost, effortless sample pre-processing, and independence from large-scale instruments. Recent studies have demonstrated LFSA can be applied to detect viral RNA. For example, Wang et al. demonstrate a lateral flow strip for the detection of severe acute respiratory syndrome coronavirus 2 (SARS-CoV-2) RNA, using S9.6-monoclonal antibody-labeled fluorescent nanoparticles to capture the RNA-DNA hybrids.<sup>24</sup> Inspired by previous research studies, we expand gold nanoparticles (AuNP)-based LFSA application with the development of a rapid, sensitive, and easy-to-use assay for qualitative and quantitative detection of dsRNA byproducts in IVT mRNA. In comparison with other methods, our platform assay achieves a rapid on-site screening of dsRNA contaminants in mRNA within 15 min. The readout can either be inspected by direct visualization or by using an optical detector. The limit of detection (LOD) for our device is 2.03 ng/mL with the linear detection range from 3 to 672 ng/mL for dsRNA contaminants in uridine (U)-containing IVT mRNA product while the LOD for dsRNA contaminants in N1-methyl-pseudouridine (m1Ψ)-containing IVT mRNA is 69.32 ng/mL with the linear detection range from 215 to 13,758 ng/

mL. Furthermore, we correlate our LFSA detection results with a series of immune response analyses in animal studies to confirm the efficacy of our device in detecting immunogenic contaminants. The results demonstrate minimal immune response in mice to the mRNA samples that tested negative on LFSA, while the increased level of interferon (IFN)- $\beta$  and interleukin (IL)-6 secretion induced by dsRNA contaminants is correlated with positive LFSA readout. Altogether, our LFSA platform allows rapid, sensitive, and quantitative monitoring of dsRNA contaminants in IVT mRNA products and can thus prevent potential immunogenicity.

## RESULTS

### Design and operation of the LFSA

The dsRNA detection mechanism in LFSA platform was based on a sandwich immunoassay. The assembled dsRNA detection test strip consisted of sample, conjugate, and absorbent pads, and a nitrocellulose (NC) membrane. The four components were partially overlaid to allow the liquid sample to pass through (Figures 1A and S1). We screened six antibody pairs by detecting both dsRNA (poly[I:C] low molecular weight [LMW]) and dsRNA (m1Ψ) and found that J5 and K1 were most suitable for dsRNA capture, immobilization, and colorimetric report (Figure S2). AuNP-labeled J5 antibodies were sprayed onto the conjugation pad for the initial dsRNA capture. Anti-dsRNA K1 antibodies were immobilized onto the test line (T-line) of the NC membrane for the J5 detected dsRNA immobilization and colorimetric report. The control line (C-line) was coated with goat anti-rabbit IgG antibodies to capture the AuNP-labeled rabbit IgG antibodies from the conjugation pad (Figure 1A).

To run the assay, mRNA samples needed to be first diluted to 50  $\mu$ L with dilution buffer (10 mM PBS [pH 7.2–7.4] containing 8 mM  $\text{Na}_2\text{HPO}_4$ , 2 mM  $\text{KH}_2\text{PO}_4$ , 136 mM NaCl and 2.6 mM KCl, 1% BSA) and loaded on the sample pad (Figure 1B). The dsRNA contaminants were captured by the AuNP-labeled J5 antibodies on the conjugate pad. As the dsRNA-J5 antibody complex flowed through the testing strip toward the absorbent pad by capillary driving force, it was immobilized by the K1 antibodies on the T-line gradually rendering a red positive band on the test strip. The AuNP-labeled rabbit IgG antibodies were captured by the anti-rabbit IgG on the C-line. After 15 min, LFSA result could be determined by naked eyes or an optical detector. A positive result exhibited two red bands on the reaction area. A negative result presented a red band on the C-line. If there was no signal on the reaction area or only one red band presented on the T-line, the test was invalid. To quantify detected dsRNA, the optical density values of the T-line and C-line could be determined by an optical detector. The ratio of T-line value to the C-line value (T/C value) could be calculated to determine the actual quantity of dsRNA.

### LFSA validation with agarose gel electrophoresis and dot-blot assay

We validated the feasibility of the LFSA for dsRNA detection by comparing with agarose gel electrophoresis and dot-blot assay. In this study, EGFP-encoded mRNA was the molecule of interest. To obtain single-stranded RNA (ssRNA) and dsRNA, we applied the

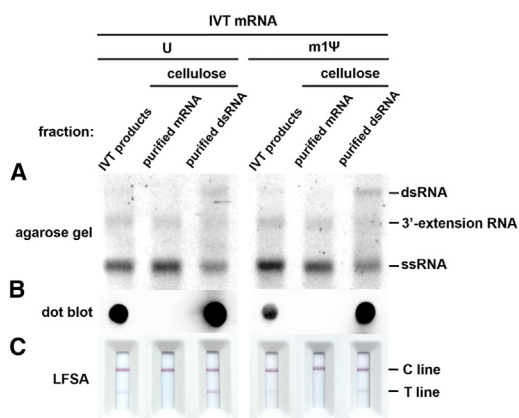


**Figure 2. LFSA validation with agarose gel electrophoresis and dot-blot assay**

EGFP-encoded mRNA products synthesized by IVT, purified mRNA, and dsRNA contaminants separated by cellulose-filled microcentrifuge spin columns were analyzed using (A) 1% native agarose gel electrophoresis, (B) dot-blot assay with J2 mAb, and (C) LFSA device.

cellulose purification technique to separate dsRNA from ssRNA in IVT mRNA products (Materials and methods). Briefly, EGFP-encoded mRNA contained with U or m1Ψ modification were synthesized by the IVT process (Materials and methods). The ssRNA and dsRNA in the IVT mRNA (U or m1Ψ) products were separated by microcentrifuge spin columns filled with microcrystal cellulose in an ethanol-containing buffer. The dsRNA bound to microcrystal cellulose in the presence of ethanol, while ssRNA eluted through the spin columns. The dsRNA was then eluted with nuclease-free water. These samples were used for LFSA validation.

We first analyzed the mRNA samples with agarose gel electrophoresis (Materials and methods; Figure 2A). As agarose gel electrophoresis had low detection sensitivity for dsRNA contaminant in IVT products, we used a large amount of RNA sample (300 ng) for agarose gel electrophoresis analysis. IVT products with both U and m1Ψ showed three bands that corresponded to dsRNA (top), 3' extension RNA (middle),<sup>25</sup> and ssRNA (bottom) (Figure 2A). However, the signal of the top bands for both U- and m1Ψ-containing IVT products was weak, suggesting agarose gel electrophoresis could barely detect dsRNA contaminant from 300 ng of IVT products. Notably, the top band was significantly reduced in purified U- and m1Ψ-containing ssRNA samples, indicating efficient dsRNA removal by cellulose purification (Figure 2A). Whereas the signal of the top bands for both purified U- and m1Ψ-containing dsRNA was more intense than it is for IVT products, suggesting a high level of dsRNA in the purified dsRNA sample. The middle and bottom bands could still be observed in purified U- and m1Ψ-containing dsRNA, which might be caused by the nonspecific binding of ssRNA and 3' extension RNA on the cellulose during the cellulose purification process.

We then performed dot-blot assay with the dsRNA specific J2 antibody to analyze the difference between RNA samples (materials

and methods). We applied 100 ng of samples for dot-blot assay. Figure 2B showed a positive signal for U- and m1Ψ-containing IVT products and purified U- and m1Ψ-containing dsRNA. A weak signal was detected for purified U- and m1Ψ-containing ssRNA. dsRNA in m1Ψ-containing IVT product showed a lower signal than in U-containing IVT product. Because the affinity of J2 antibody to both U- and m1Ψ-containing dsRNA was comparable,<sup>13</sup> the detection difference should be caused by the production of fewer dsRNA contaminants during the *in vitro* transcription process of m1Ψ-containing mRNA compared with U-containing mRNAs.<sup>26</sup> As expected, weak signal was detected in the purified ssRNA, which further confirmed the efficient removal of dsRNA contaminants by the cellulose purification method.

We finally evaluated the detection performance of the LFSA device by using the test strip to detect 100 ng of mRNA samples (materials and methods; Figure 2C). When testing the IVT products, the test strip displayed two red bands, indicating that the IVT products contained dsRNA contaminants. The test strip showed a single C-line for the purified ssRNA sample while showing two lines for the purified dsRNA sample in accordance with the results from agarose gel electrophoresis and dot-blot assay. Notably, the T-line signal was more pronounced for U-containing mRNA samples than for m1Ψ-containing mRNA samples, which was similar to the results of dot-blot assay.

#### Specificity assay and interference assay of the LFSA device for dsRNA detection

High specificity was essential for dsRNA detection, as any error could result in low-quality mRNA for research and pharmaceutical applications. Thus, we examined whether the mAbs were specific to dsRNA by adding various forms and concentrations of nucleic acids that had similar or same chemical compositions to dsRNA (detailed sequences are shown in Table S1).

We first tested whether the mAbs were able to distinguish dsRNA from other forms of nucleic acids. Ten micrograms per milliliter of different forms of nucleic acids including ssDNA primer, dsDNA PCR product, DNA plasmid, U- and m1Ψ-containing ssRNA, and 1 μg/mL of U- and m1Ψ-containing dsRNA, were serially tested using the LFSA (Figure 3A). Poly(I:C) LMW (0.2–1 kb) was used as a positive control. The results showed a minimal optical reading signal for all tested samples except for purified U- and m1Ψ-containing dsRNA and poly(I:C) LMW. In addition, there was no cross-reactivity with other forms of nucleic acids. LFSA detection signal for m1Ψ-containing dsRNA showed relatively lower than for an equal concentration of U-containing dsRNA.

As the chemical composition of the ssRNA was similar to dsRNA, ssRNA might interfere with the binding of dsRNA to the antibody. Therefore, we studied if the presence of ssRNA affected dsRNA detection in the LFSA. We applied LFSA to detect 34 ng/mL U- and m1Ψ-containing dsRNA with ssRNA in increasing ratios. The dsRNA/ssRNA concentration ratios of 1:100, 1:200, 1:500, and

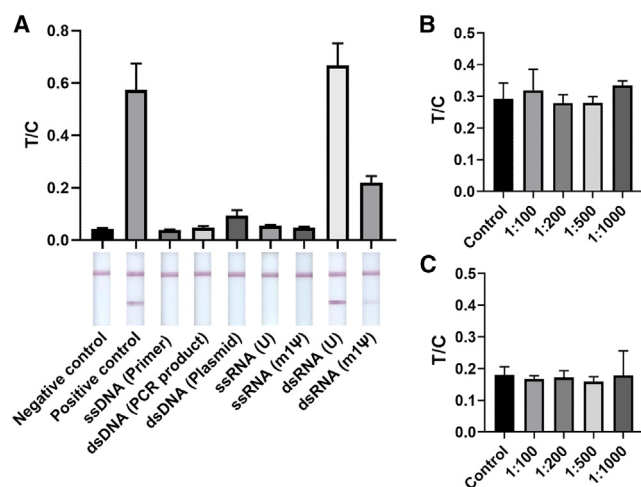


**Figure 3. Specificity assay and interference assay of the LFSA device for dsRNA detection**

(A) Histograms of the detected T/C value of different nucleic acids and analogs (1  $\mu\text{g/mL}$  for positive control [poly(I:C) LMW], U- and m1 $\Psi$ -containing dsRNA; 10  $\mu\text{g/mL}$  for all other nucleic acids), as well as photos of lateral flow strips. (B) The interference assay of the LFSA for 34 ng/mL of U-containing dsRNA detection at different dsRNA/ssRNA concentration ratios (1:100, 1:200, 1:500, 1:1,000). (C) The interference assay of the LFSA for 34 ng/mL of m1 $\Psi$ -containing dsRNA detection at different dsRNA/ssRNA concentration ratios (1:100, 1:200, 1:500, and 1:1,000). The error bars represent the SD of experimental triplicates. Data are represented as mean  $\pm$  SD. \* $p < 0.05$ , \*\* $p < 0.01$ , and \*\*\* $p < 0.001$ , according to the paired two-tailed *t*-test comparison of every group and control group.

1:1,000 were analyzed. The results showed no statistically significant difference, indicating that ssRNA had limited interference to LFSA (Figures 3B and 3C). In addition, we evaluated the highest loading amount of IVT mRNA on the test strip. The results showed that the test strip can load up to 2  $\mu\text{g}$  of sample (Figure S3).

#### Quantitative detection of the LFSA device

Standard curves were generated for dsRNA detection to achieve quantitative analysis. We first evaluated the quantitative detection performance of our LFSA platform using complete complementary dsRNA with the same mRNA molecular length of EGFP, luciferase, and Cas9 (materials and methods; Figures S4 and S5). As reported previously, dsRNA length influenced the binding affinity of mAb which could directly affect our LFSA for dsRNA detection.<sup>15,27</sup> To obtain a general picture of the linear detection range for long dsRNA and short dsRNA, we also generated the standard curves for both poly(I:C) LMW (0.2–1 kb) and poly(I:C) HMW (high molecular weight; 1.5–8 kb). A series of dilutions of different dsRNA standards were loaded onto the sample pad of test strips for analysis. The LFSA test results were quantified by measuring the optical density values of the T-line and C-line with a colloidal gold optical detector (Figure S1). The calculated average T/C values for the dilution series of dsRNA standards were presented in both scatter graphs (Figure 4) and heatmaps (Figure S6). The LOD value and linear detection range for U-containing dsRNA, m1 $\Psi$ -containing dsRNA, poly(I:C) LMW,

and poly(I:C) HMW were listed in Table 1. Notably, the hook effect started to show when the titers of samples of corresponding dsRNA standards exceeded 2,687, 13,758, 537, and 2,150 ng/mL.<sup>28</sup> The non-linear regions appearing on the curve was the postzone phenomenon in the hook effect, which is caused by excess antigens occupying the binding sites of detection antibody and capture antibody, resulting in the reduction of immune complexes. This hook effect could be observed in the heatmaps as well (Figure S6).

#### Correlation between the LFSA test results and the immune response caused by dsRNA in mice

We correlated the LFSA test results of different dosages of m1 $\Psi$ -containing dsRNA standard and IVT mRNA before and after purification with their animal immune response analysis to confirm that LFSA testing could estimate the immune response (Figure 5).

We measured the levels of IFN- $\beta$  and IL-6, as the common factors of immediate immune response, 6 h post-injection of mRNA samples.<sup>29,30</sup> m1 $\Psi$ -containing dsRNA standards of 0.017, 0.17, and 1.7  $\mu\text{g}$  were used for quantitative LFSA and animal immune response analysis (Figures 5A–5C). LFSA quantitative analysis confirmed the amounts of dsRNA as those intended to be used in the experimental design. The levels of IFN- $\beta$  and IL-6 in mice increased proportionally with m1 $\Psi$ -containing dsRNA, affirming a direct correlation between the amount of dsRNA and the two immune response factors.

Furthermore, we applied LFSA to detect the amount of dsRNA in IVT mRNA samples and confirmed that the immune response from these contaminated IVT mRNA samples was reduced after cellulose purification. The LFSA test suggested there is about  $58.02 \pm 11.41$  ng of dsRNA in 10  $\mu\text{g}$  IVT mRNA (Figure 5D). As expected, the purified IVT mRNA was negative on LFSA. The levels of IFN- $\beta$  and IL-6 increased after injection of unpurified IVT mRNA, indicating an acute immune response (Figures 5E and 5F). Both IFN- $\beta$  and IL-6 dropped for purified IVT mRNA, suggesting the removal of dsRNA reduces the immune response (Figures 5E and 5F). Notably, even with the purification, the level of IL-6 slightly increased (Figure 5F), which could be due to the cellulose purification technique not having fully removed the dsRNA contaminants, and the remaining dsRNA contaminants were likely to induce a minor secretion of IL-6 (Figure 5F). We found that 0.17  $\mu\text{g}$  pure dsRNA induced about 10 pg/mL IL-6 (Figure 5C) and 10  $\mu\text{g}$  of unpurified IVT mRNA that contained about 58.02 ng dsRNA (Figure 5D) led to a 6-fold stronger IL-6 response (Figure 5F). This contradicting result might be caused by the structural difference between dsRNA contaminants from IVT products and pure dsRNA standards. The dsRNA standards we prepared were the complete complementary dsRNA (sense-antisense), while the dsRNA produced by IVT contains multiple structures, such as abortive transcripts,<sup>5</sup> dsRNA (3'-extended) product,<sup>6</sup> and dsRNA (sense-antisense).<sup>7</sup>

#### DISCUSSION

Fast and precise on-site detection technology provides convenient method for quality control of biological products. We expand the

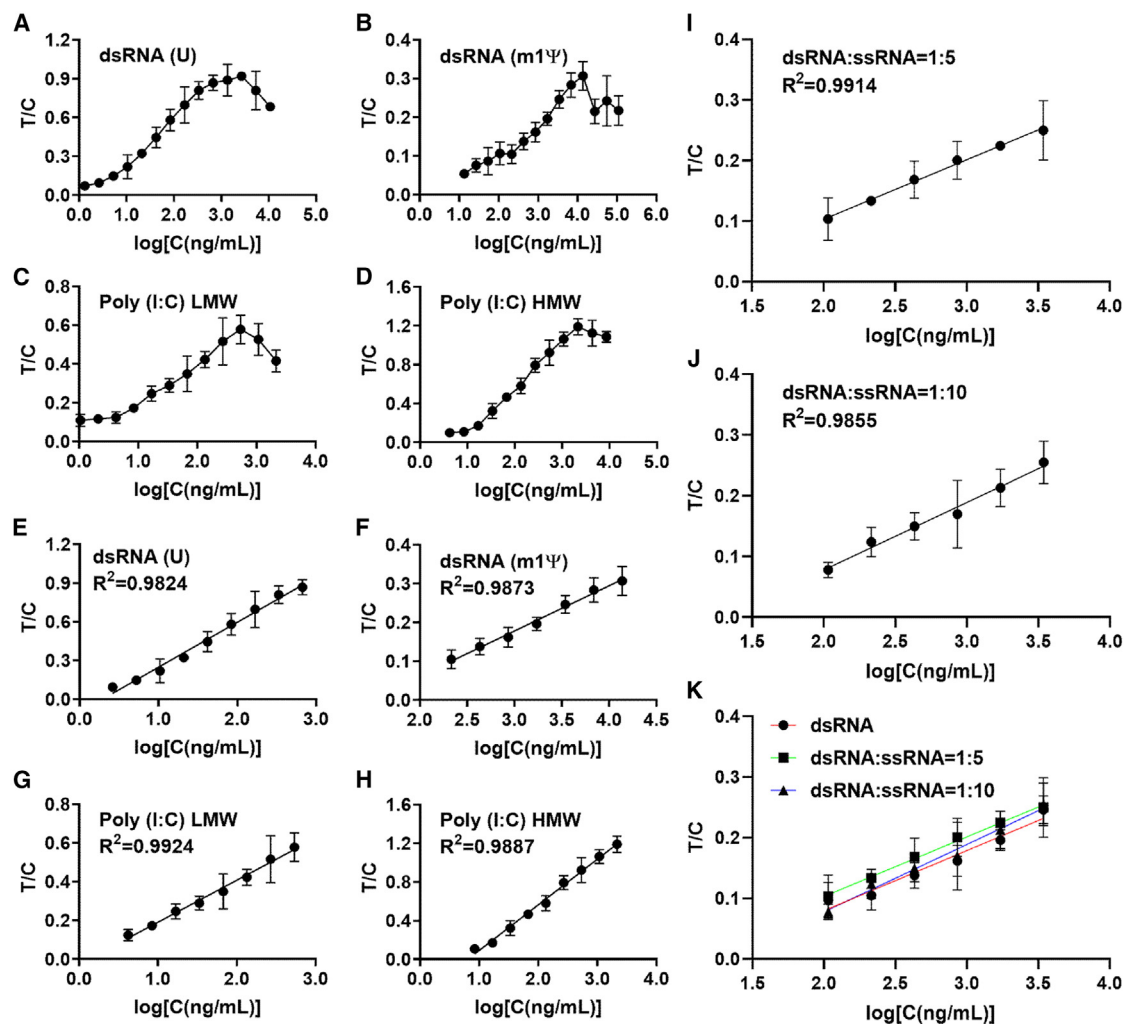


**Figure 4. Sensitivity assay of the LFSA device for the quantification of dsRNA standards**

Scatterplot of the T/C value as a function of the concentration of (A) U-containing dsRNA (880 bp), (B) m1Ψ-containing dsRNA (880 bp), (C) poly(I:C) LMW, and (D) poly(I:C) HMW. The linear relationship between the T/C value and the concentration of (E) U-containing dsRNA, (F) m1Ψ-containing dsRNA, (G) poly(I:C) LMW, and (H) poly(I:C) HMW. The linear relationship between the T/C value and the concentration of m1Ψ-containing dsRNA at dsRNA/ssRNA concentration ratio of (I) 1:5 and (J) 1:10. (K) The linear relationship between the T/C value and the concentration of m1Ψ-containing dsRNA at the absence and presence of ssRNA. The error bars represent the SD of experimental triplicates.

application of LFSA for the detection of dsRNA, which is the primary IVT contaminant and the key activator of triggering innate immune responses.

In this study, we applied three methods, including agarose gel electrophoresis, dot-blot assay, and LFSA, to detect dsRNA contaminants in IVT mRNA products (Figure 2), and compared the detection capability of these methods (Table 2). For the detection time, agarose gel electrophoresis needs at least 1 h, including the gel preparation, sample loading, running the gel, and visualization; dot-blot assay needs 4–5 h, including sample loading, membrane blocking, primary and secondary antibody incubation, membrane washing, and visualization. In contrast, our LFSA can complete the procedures of sample

dilution, loading, and observation within 15 min, which is 4 times faster than agarose gel electrophoresis and 16 times faster than dot-blot assay (Table 2). From the aspect of sensitivity, agarose gel electrophoresis employs fluorescence visualization, but it has low sensitivity and resolution for trace amounts of dsRNA. Dot-blot assay is sensitive for trace amounts of dsRNA in IVT samples on the basis of chemiluminescent method, which is comparable with our LFSA that can detect ng quantities of dsRNA by the colorimetric method. From the aspect of specificity, in comparison with dot-blot assay, our LFSA maintains high specificity which is based on the recognition of antibodies to dsRNA (Figure 3A). Moreover, for qualitative analysis, LFSA does not require any imaging instruments to observe the results. Notably, high-performance liquid chromatography (HPLC)

**Table 1. Limit of detection and linear detection range for different dsRNA standards detection by LFSA**

Detection substance	Limit of detection, ng/mL	Linear detection range, ng/mL
U-containing dsRNA	2.03	3–672
m1Ψ-containing dsRNA	69.32	215–13,758
Poly(I:C) LMW	2.28	4–537
Poly(I:C) HMW	7.53	8–2,150

is a common sensitive analytical tool. Ion pair reverse-phase HPLC (IP-RP-HPLC) has been previously shown to separate ssRNA from corresponding dsRNA.<sup>31</sup> Previous report also applied HPLC to remove dsRNA from mRNA.<sup>32</sup> However, no literature reports that HPLC can accurately quantify dsRNA from IVT. Thus, in terms of detection duration, sensitivity, and specificity, our LFSA is a great alternative to existing technology and greatly meets the requirements for dsRNA detection.

The quantitative detection of dsRNA can be achieved by using a colloidal gold optical detector (Figures 4 and S8). If the optical detector is not available, quantitative analysis can be conducted through imaging analysis software under proper experimental conditions.<sup>33–35</sup> Different dsRNA standards were used for establishing standard curves (Figures 4E–4H). Determined from the standard curves, LFSA can detect as low as 2.03 ng/mL of U-containing dsRNA and 69.32 ng/mL of m1Ψ-containing dsRNA. LFSA has higher sensitivity to U-containing dsRNA, as the capture antibody (K1) shows stronger binding to U-containing dsRNA (Figure S9).<sup>15</sup>

To examine whether the standard curve established by pure dsRNA standard is consistent with the standard curve established in the presence of ssRNA, we have set up the m1Ψ-containing dsRNA standard curves in the presence of ssRNA with the dsRNA/ssRNA concentration ratio of 1:5 and 1:10 (Figures 4I and 4J). The standard curves with the two dsRNA/ssRNA concentration ratios have no significant difference from the pure dsRNA standard curve, indicating that the standard curve established by pure dsRNA standard is suitable for the quantification of dsRNA in actual samples (Figure 4K). Together, our results suggest LFSA can quantitatively detect dsRNA in *in vitro*-transcribed mRNA samples.

## Conclusion

We have developed a colloidal gold nanoparticle-based lateral flow strip device for the detection of dsRNA contaminants in IVT mRNA products. Compared with the traditional detection methods, such as agarose gel electrophoresis and dot-blot assay, LFSA offers a rapid, sensitive, and simple-to-use solution. LFSA provides not only qualitative dsRNA detection but also quantitative dsRNA analysis when coupled with an optical detector. The animal immune response analysis also confirms that LFSA constitutes an early warning method for the immune response due to dsRNA contamination. Given the increasing interest in mRNA-related research, vaccines,

and the pharmaceutical industry, high-purity mRNA products are in great demand. Various detection means are essential for mRNA quality control. We believe the LFSA that allows rapid, sensitive, and simple-to-use detection has the potential to replace dot-blot assay and will tremendously facilitate mRNA research progress and manufacture.

## MATERIALS AND METHODS

### Preparation of AuNP-labeled anti-dsRNA J5 antibody

Colloidal gold nanoparticles (AuNPs) (diameter 30 nm) were synthesized by the trisodium citrate reduction method.<sup>36</sup> The morphology of colloidal gold nanoparticles was characterized by the JEM-2100F transmission electron microscope (JEOL). The ultraviolet-visible (UV-Vis) absorption spectra of colloidal gold nanoparticles were recorded by the NanoDrop One spectrophotometer (Thermo Fisher Scientific). The dynamic light scattering (DLS) analyses and zeta potentials of colloidal gold nanoparticles were collected by the Zetasizer Ultra (Malvern Panalytical, Shanghai, China). AuNPs were coated with anti-dsRNA J5 antibody (Nordic-MUBio, Susteren, the Netherlands) by adjusting pH to about 8.0. Briefly, 16 μL 0.2 M potassium carbonate (Sinopharm, Beijing, China) was added to 2 mL AuNPs solution. Twenty microliters of J5 mAb solution (1.0 mg/mL) was added to AuNPs solution with standing for 5 min. Then 20 μL 20% BSA (10 mM Tris-HCl [pH 8.0]) (Proliant) solution was added to block nonspecific sites and stabilize the AuNP-mAb conjugate. The solution was centrifuged at 20,000 rpm for 5 min at 4°C. The supernatant was discarded, and the precipitate was resuspended by 120 μL resuspension buffer (10 mM Tris-HCl [pH 8.0], 0.05% Tween 20, 1% BSA, and 5% sucrose), then ultrasonic dispersion. Finally, 3 μL AuNP-labeled rabbit IgG mAb (Genstars, Nanjing, China) solution was vortex with 120 μL AuNP-labeled anti-dsRNA J5 mAb solution before use. Characterizations of AuNPs and AuNP-mAb are shown in Figure S10.

### Purification of IVT mRNA

mRNAs were transcribed from linearized plasmids encoding EGFP, luciferase, and Cas9 by T7 High Yield RNA Transcription Kit (Vazyme). The plasmids encoding EGFP, luciferase, and Cas9 had been subjected to Sanger sequencing. The detailed sequences of the plasmids encoding EGFP, luciferase, and Cas9 were provided in Table S2. The transcription reaction generated two types of nucleoside-containing mRNAs. All components were incubated at 37°C for 2 h before DNase I (Vazyme) digestion. Then the synthesized mRNA was purified by the magnetic beads (Vazyme). Separation of dsRNA byproducts from single-stranded mRNA was performed by cellulose-based purification process, as previously described.<sup>13</sup> In brief, 100 μg IVT mRNA in 500 μL loading buffer (10 mM HEPES [pH 7.2], 0.1 mM EDTA, 125 mM NaCl, and 16% [v/v] ethanol) was added to the spin column filled with the prewashed cellulose. IVT mRNA and cellulose mixture were shaken vigorously at room temperature for 30 min to promote the binding of dsRNA to cellulose. By centrifugation at 14,000 g for 60 s, the unbound single-stranded mRNA flowed out with the effluent and separated from dsRNA. To substantially remove dsRNA, the above flowthrough needed to go through the column again.

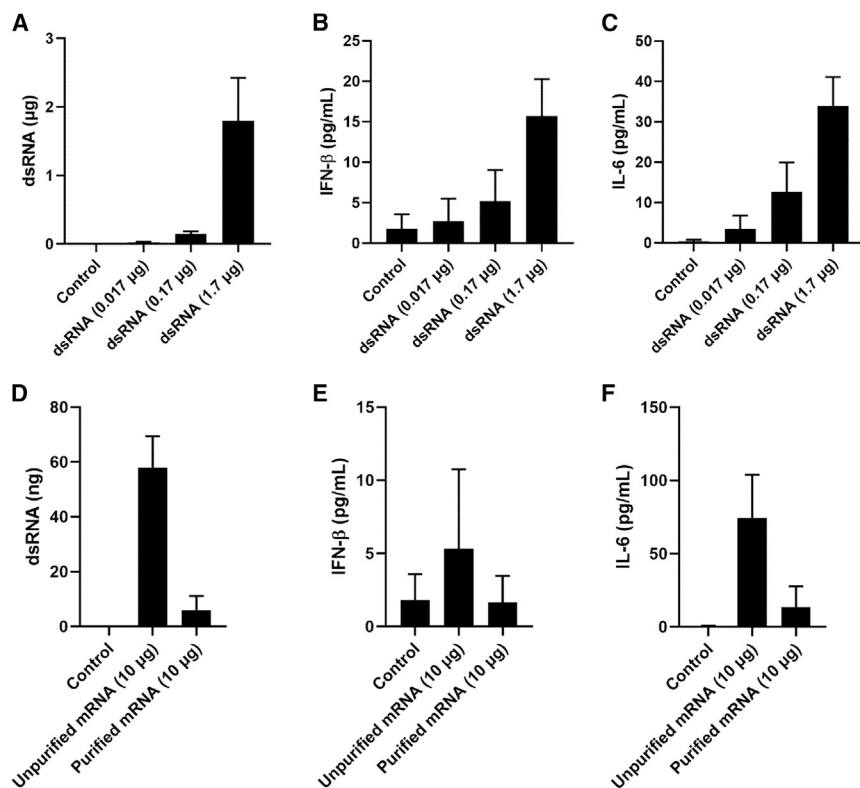


**Figure 5. Relationship between LFSA result and the immune response of dsRNA**

(A) Histograms of the converted amount of m1Ψ-containing dsRNA. (B) IFN-β secretion was measured at 6 h after injection intravenously with 0.017, 0.17, and 1.7 μg of m1Ψ-containing dsRNA. (C) IL-6 secretion was measured at 6 h after intravenous injection with 0.017, 0.17, and 1.7 μg of m1Ψ-containing dsRNA. (D) Histograms of the converted amount of m1Ψ-containing dsRNA in IVT mRNA before and after purification (10 μg). (E) IFN-β secretion was measured at 6 h after intravenous injection with 10 μg of m1Ψ-containing unpurified and purified mRNA. (F) IL-6 secretion was measured at 6 h after intravenous injection with 10 μg of m1Ψ-containing unpurified and purified mRNA. The error bars represent the SD of experimental triplicates.

The concentration of IVT mRNA was determined by the NanoDrop One spectrophotometer (Thermo Fisher Scientific) using commonly the value of 40 μg/mL/A<sub>260</sub>.<sup>37,38</sup> The integrity of transcripts was analyzed by 1% native agarose gel electrophoresis.

#### Preparation of dsRNA standards

Plasmids encoding EGFP, luciferase, and Cas9 were used as PCR templates. Templates with the forward or reverse T7 promoter for *in vitro* transcription were prepared by PCRs. Complementary U- or m1Ψ-containing RNAs were *in vitro* transcribed. Annealing of the complementary strands was performed by heating to 95°C for 1 min in buffer (10 mM Tris-HCl [pH 7.0], 50 mM NaCl) and cooling to room temperature for 2 h. The sequences of designed primers for the preparation of dsRNA standards are listed in Table S2. We used a value of 46.52 μg/mL/A<sub>260</sub> for the quantification of the standard control dsRNA samples referring to recent publications.<sup>38,39</sup>

#### Preparation of test strips

##### Treatment of test strips

The sample pad (Jinbiao, Shanghai, China) and conjugation pad (Jinbiao) were immersed with the treatment buffer for 5 min, dried at 25°C for 2 h, and finally stored in a cool and dry place. AuNP-labeled mAb mixture solution containing AuNP-labeled J5 mAb and AuNP-labeled rabbit IgG mAb (OD<sub>520</sub> = 0.36, after 20-fold dilution) was sprayed to the conjugation pad with the rate of 4.1 μL/cm using an XYZ 3D film spraying instrument-HM3035 (Jinbiao), dried at 25°C

for 4–5 h. Anti-dsRNA K1 antibody (1.0 mg/mL) (Nordic-MUBio) and goat anti-rabbit IgG antibody (1.5 mg/mL) (Genstars) were sprayed to the test line and control line on the NC membrane (Millipore), at a rate of 1 μL/cm, dried at 25°C for 2 h, and finally stored in a cool and dry place.

##### Assembly of test strips

The absorption pad (Jinbiao), NC membrane, conjugation pad, and sample pad were assembled on the polyvinyl chloride (PVC) adhesive pad (Jinbiao), arranged in sequence and each part overlaps by 2 mm, with the NC membrane at the bottom. The assembled strips were cut to 3 mm width by Strip cutter-CTS300 (Jinbiao) before use.

##### Lateral flow strip assay

The optical density values of the T-line and C-line were determined with a colloidal gold reader (Anbio, Xiamen, China). The sensitivity of the strips for detecting dsRNA was determined by adding 50 μL of serially diluted standard samples. The LOD was calculated from the fitting equation, in which the T/C values were used as the vertical axis and the logarithm concentration of dsRNA as the horizontal axis. Specifically, the mean value of negative controls (0 ng/mL of dsRNA standard) plus three times the standard deviation substitutes into the fitting equation ( $Y = aX + b$ ,  $[X = \lg C]$ ) and obtain the value of LOD.<sup>40</sup> The specificity of the strips was identified by 10 μg/mL of other nucleic acids (U- or m1Ψ-containing ssRNA, ssDNA, dsDNA) and 1 μg/mL synthetic dsRNA (poly[I:C] LMW) (Invitrogen, Shanghai, China).

##### Dot-blot assay

Ten microliters of dsRNA standards containing 0.1, 1, 10, 100, and 1,000 ng/μL were added to the polyvinylidene difluoride (PVDF) membrane (Amersham, Shanghai, China), which was activated by 100% methanol. After loading, the PVDF membrane was blocked in TBS-T buffer containing 5% (w/v) non-fat dried milk

**Table 2. Summary of the analytical performance for dsRNA detection with different methods**

	HPLC	Agarose gel electrophoresis	ELISA	Dot blot	LFSA
Assay time	2–4 h	1 h	7–8 h	4–5 h	15 min
Sensitivity	low	low	high	high	high
Specificity	low	low	high	high	high
Experimental environment	laboratory	laboratory	laboratory	laboratory	on-site
Operation	complex	easy	complex	complex	easy
Readout	N/A	qualitative	qualitative quantitative	qualitative semi-quantitative	qualitative quantitative
Equipment	precision instrument	electrophoresis device	precision instrument	precision instrument	portable device

(BD-Difco). The membrane was incubated with anti-dsRNA J2 mAb (1:7,000 diluted by TBS-T buffer containing 1% [w/v] non-fat milk powder) for 1 h, then washed with 10 mL TBS-T buffer for 10 min. After washing four times, the membrane was incubated with HRP-conjugated goat anti-mouse IgG (Easybio, Beijing, China) (1:7,000 diluted by TBS-T buffer containing 1% (w/v) non-fat dried milk) for 1 h. After washing four times, the signal was detected by adding chemiluminescent reagents (Bridgen) and imaged on the ChemiDoc MP Imaging System (Bio-Rad).

#### Ion pair reverse-phase high-performance liquid chromatography assay

RNA samples were analyzed by HPLC (Agilent 1260) using a DNAPac RP, analytical column (4  $\mu$ m, 2.1  $\times$  100 mm; Thermo Fisher Scientific) at 260 nm. The chromatographic analysis was performed using the following conditions: buffer A: 0.1 M triethylamine acetate (TEAA) (pH 7.0); buffer B: 0.1 M TEAA (pH 7.0), containing 75% acetonitrile and 25% H<sub>2</sub>O. The gradient started at 7% buffer B and remained for 10 min, followed by a linear extension to 40% buffer B over 30 min, then to 45% buffer B over 5 min. The system flow rate was set as 0.2 mL/min and the column temperature was 50°C.

#### Animal experiments

All animal studies were approved by the Laboratory Animal Management Committee of Chinese Academy of Sciences (approval number APIMCAS2021011). Female BALB/c mice were used from the Institute of Microbiology Chinese Academy of Sciences. To determine the immunogenicity of dsRNA standards and IVT mRNA before and after cellulose purification, different RNA samples were diluted with 10 mM PBS (pH 7.2–7.4) containing 8 mM Na<sub>2</sub>HPO<sub>4</sub>, 2 mM KH<sub>2</sub>PO<sub>4</sub>, 136 mM NaCl, and 2.6 mM KCl (Solarbio, Beijing, China) and injected intravenously as naked RNA into mice (3 mice/group). Blood was harvested after 6 h and to obtain serum by centrifugation at 1,000  $\times$  g for 10 min. The levels of IFN- $\beta$  and IL-6 were measured using ELISA kit (BioLegend, Beijing, China) and CLARIOstar Plus plate reader (BMG LABTECH).

#### Statistical analysis

Data were statistically analyzed using OriginPro software (OriginLab, Northampton, MA) and Prism 8.0 software (GraphPad, San Diego, CA). All data are presented as mean  $\pm$  SD of at least three indepen-

dent experiments. One-way ANOVA and paired *t* tests were performed for comparisons between groups. A *p* value <0.05 was considered to indicate statistical significance. Figures 1 and S1 were created using BioRender.com.

#### DATA AVAILABILITY

All data included in this study are available upon request by contact with the corresponding author.

#### SUPPLEMENTAL INFORMATION

Supplemental information can be found online at <https://doi.org/10.1016/j.omtn.2023.04.005>.

#### ACKNOWLEDGMENTS

This work was financially supported by the Chinese Academy of Science (CAS) Project for Young Scientists in Basic Research (YSBR010).

#### AUTHOR CONTRIBUTIONS

D.L., Z.W., D.X., and Y.C. designed the experiments. D.L., J.Z., and F.S. performed the experiments. D.W., S.W., S.C.-B., D.X., and Y.C. conducted the experiments. D.L., Z.W., and F.S. analyzed the data and prepared the figures. D.L. and Z.W. wrote the manuscript. D.X. and Y.C. amended the manuscript. All authors reviewed the manuscript, and the manuscript was approved by all authors for publication.

#### DECLARATION OF INTERESTS

The authors declare no competing interests.

#### REFERENCES

- Machado, B.A.S., Hodel, K.V.S., Fonseca, L.M.d.S., Mascarenhas, L.A.B., Andrade, L.P.C.d.S., Rocha, V.P.C., Soares, M.B.P., Berglund, P., Duthie, M.S., et al. (2021). The importance of RNA-based vaccines in the fight against COVID-19: an overview. *Vaccines* 9, 1345.
- Mu, Z., Haynes, B.F., and Cain, D.W. (2021). HIV mRNA vaccines—progress and future paths. *Vaccines* 9, 134.
- Beckert, B., and Masquida, B. (2011). Synthesis of RNA by *in vitro* transcription. *Methods Mol. Biol.* 703, 29–41.
- Dolgin, E. (2021). The tangled history of mRNA vaccines. *Nature* 597, 318–324.
- Milligan, J.F., Groebe, D.R., Witherell, G.W., and Uhlenbeck, O.C. (1987). Oligoribonucleotide synthesis using T7 RNA polymerase and synthetic DNA templates. *Nucleic Acids Res.* 15, 8783–8798.



6. Triana-Alonso, F.J., Dabrowski, M., Wadzack, J., and Nierhaus, K.H. (1995). Self-coded 3'-extension of run-off transcripts produces aberrant products during *in vitro* transcription with T7 RNA polymerase. *J. Biol. Chem.* *270*, 6298–6307.
7. Nacheva, G.A., and Berzal-Herranz, A. (2003). Preventing undesired RNA-primed RNA extension catalyzed by T7 RNA polymerase. *Eur. J. Biochem.* *270*, 1458–1465.
8. Alexopoulou, L., Holt, A.C., Medzhitov, R., and Flavell, R.A. (2001). Recognition of double-stranded RNA and activation of NF- $\kappa$ B by Toll-like receptor 3. *Nature* *413*, 732–738.
9. Barral, P.M., Sarkar, D., Su, Z.Z., Barber, G.N., DeSalle, R., Racaniello, V.R., and Fisher, P.B. (2009). Functions of the cytoplasmic RNA sensors RIG-I and MDA-5: key regulators of innate immunity. *Pharmacol. Ther.* *124*, 219–234.
10. Mu, X., and Hur, S. (2021). Immunogenicity of *in vitro*-transcribed RNA. *Acc. Chem. Res.* *54*, 4012–4023.
11. Han, J., Zhong, C.Q., and Zhang, D.W. (2011). Programmed necrosis: backup to and competitor with apoptosis in the immune system. *Nat. Immunol.* *12*, 1143–1149.
12. Tuschl, T., Zamore, P.D., Lehmann, R., Bartel, D.P., and Sharp, P.A. (1999). Targeted mRNA degradation by double-stranded RNA *in vitro*. *Genes Dev.* *13*, 3191–3197.
13. Baiersdörfer, M., Boros, G., Muramatsu, H., Mahiny, A., Vlatkovic, I., Sahin, U., and Karikó, K. (2019). A facile method for the removal of dsRNA contaminant from *in vitro*-transcribed mRNA. *Mol. Ther. Nucleic Acids* *15*, 26–35.
14. Nelson, J., Sorensen, E.W., Mintri, S., Rabideau, A.E., Zheng, W., Besin, G., Khatwani, N., Su, S.V., Miracco, E.J., Issa, W.J., et al. (2020). Impact of mRNA chemistry and manufacturing process on innate immune activation. *Sci. Adv.* *6*, eaaz6893.
15. Schönborn, J., Oberstraß, J., Breyel, E., Tittgen, J., Schumacher, J., and Lukacs, N. (1991). Monoclonal antibodies to double-stranded RNA as probes of RNA structure in crude nucleic acid extracts. *Nucleic Acids Res.* *19*, 2993–3000.
16. Fass, D., Kemp, M., Schroeder, F., Wagner, F., Wang, Q., and Holson, E. (2012). Epigenetics Regulation and Epigenomics: Advances in Molecular Biology and Medicine (Weinheim, Germany: Wiley-VCH-Verlag & Co. KGaA).
17. Tansley, S.L., Li, D., Betteridge, Z.E., and McHugh, N.J. (2020). The reliability of immunoassays to detect autoantibodies in patients with myositis is dependent on auto-antibody specificity. *Rheumatology* *59*, 2109–2114.
18. Joung, J., Ladha, A., Saito, M., Kim, N.-G., Woolley, A.E., Segel, M., Barretto, R.P.J., Ranu, A., Macrae, R.K., Faure, G., et al. (2020). Detection of SARS-CoV-2 with SHERLOCK one-pot testing. *N. Engl. J. Med.* *383*, 1492–1494.
19. Kellner, M.J., Koob, J.G., Gootenberg, J.S., Abudayyeh, O.O., and Zhang, F. (2019). SHERLOCK: nucleic acid detection with CRISPR nucleases. *Nat. Protoc.* *14*, 2986–3012.
20. Yao, J., Wang, Z., Guo, L., Xu, X., Liu, L., Kuang, H., and Xu, C. (2021). Lateral flow immunoassay for the simultaneous detection of fipronil and its metabolites in food samples. *Food Chem.* *356*, 129710.
21. Sheng, E., Lu, Y., Xiao, Y., Li, Z., Wang, H., and Dai, Z. (2021). Simultaneous and ultrasensitive detection of three pesticides using a surface-enhanced Raman scattering-based lateral flow assay test strip. *Biosens. Bioelectron.* *181*, 113149.
22. Koczula, K.M., and Gallotta, A. (2016). Lateral flow assays. *Essays Biochem.* *60*, 111–120.
23. Mak, W.C., Beni, V., and Turner, A.P. (2016). Lateral-flow technology: from visual to instrumental. *TrAC Trends in Anal. Chem.* *79*, 297–305.
24. Wang, D., He, S., Wang, X., Yan, Y., Liu, J., Wu, S., Liu, S., Lei, Y., Chen, M., Li, L., et al. (2020). Rapid lateral flow immunoassay for the fluorescence detection of SARS-CoV-2 RNA. *Nat. Biomed. Eng.* *4*, 1150–1158.
25. Wu, M.Z., Asahara, H., Tzertzinis, G., and Roy, B. (2020). Synthesis of low immunogenicity RNA with high-temperature *in vitro* transcription. *RNA* *26*, 345–360.
26. Mu, X., Greenwald, E., Ahmad, S., and Hur, S. (2018). An origin of the immunogenicity of *in vitro* transcribed RNA. *Nucleic Acids Res.* *46*, 5239–5249.
27. Bonin, M., Oberstrass, J., Lukacs, N., Ewert, K., Oesterschulze, E., Kassing, R., and Nellen, W. (2000). Determination of preferential binding sites for anti-dsRNA antibodies on double-stranded RNA by scanning force microscopy. *RNA* *6*, 563–570.
28. Fernando, S.A., and Wilson, G.S. (1992). Studies of the 'hook' effect in the one-step sandwich immunoassay. *J. Immunol. Methods* *151*, 47–66.
29. Moradian, H., Roch, T., Anthofer, L., Lendlein, A., and Gossen, M. (2022). Chemical modification of uridine modulates mRNA-mediated proinflammatory and antiviral response in primary human macrophages. *Mol. Ther. Nucleic Acids* *27*, 854–869.
30. Kasuga, Y., Zhu, B., Jang, K.J., and Yoo, J.S. (2021). Innate immune sensing of coronavirus and viral evasion strategies. *Exp. Mol. Med.* *53*, 723–736.
31. Nwokeoji, A.O., Kung, A.W., Kilby, P.M., Portwood, D.E., and Dickman, M.J. (2017). Purification and characterisation of dsRNA using ion pair reverse phase chromatography and mass spectrometry. *J. Chromatogr. A* *1484*, 14–25.
32. Kariko, K., Muramatsu, H., Ludwig, J., and Weissman, D. (2011). Generating the optimal mRNA for therapy: HPLC purification eliminates immune activation and improves translation of nucleoside-modified, protein-encoding mRNA. *Nucleic Acids Res.* *39*, e142.
33. Shah, K.G., Singh, V., Kauffman, P.C., Abe, K., and Yager, P. (2018). Mobile phone ratiometric imaging enables highly sensitive fluorescence lateral flow immunoassays without external optical filters. *Anal. Chem.* *90*, 6967–6974.
34. Li, D., Huang, M., Shi, Z., Huang, L., Jin, J., Jiang, C., Yu, W., Guo, Z., and Wang, J. (2022). Ultrasensitive competitive lateral flow immunoassay with visual semiquantitative inspection and flexible quantification capabilities. *Anal. Chem.* *94*, 2996–3004.
35. Brangel, P., Sobarzo, A., Parolo, C., Miller, B.S., Howes, P.D., Gelkop, S., Lutwama, J.J., Dye, J.M., McKendry, R.A., Lobel, L., et al. (2018). A serological point-of-care test for the detection of IgG antibodies against Ebola virus in human survivors. *ACS Nano* *12*, 63–73.
36. Verma, H.N., Singh, P., and Chavan, R.M. (2014). Gold nanoparticle: synthesis and characterization. *Vet. World* *7*, 72–77.
37. Sambrook, J., and Russell, D. (2001). *Molecular Cloning: A Laboratory Manual* (3-Volume Set), Cold Spring Harbor: CSHLP 2006, pdb.prot4538.
38. Nwokeoji, A.O., Kilby, P.M., Portwood, D.E., and Dickman, M.J. (2017). Accurate quantification of nucleic acids using hypochromicity measurements in conjunction with UV spectrophotometry. *Anal. Chem.* *89*, 13567–13574.
39. Nwokeoji, A.O., Kumar, S., Kilby, P.M., Portwood, D.E., Hobbs, J.K., and Dickman, M.J. (2019). Analysis of long dsRNA produced *in vitro* and *in vivo* using atomic force microscopy in conjunction with ion-pair reverse-phase HPLC. *Analyst* *144*, 4985–4994.
40. Lee, J.H., Choi, M., Jung, Y., Lee, S.K., Lee, C.S., Kim, J., Kim, J., Kim, N.H., Kim, B.T., and Kim, H.G. (2021). A novel rapid detection for SARS-CoV-2 spike 1 antigens using human angiotensin converting enzyme 2 (ACE2). *Biosens. Bioelectron.* *171*, 112715.